We are IntechOpen, the world's leading publisher of Open Access books
Built by scientists, for scientists

6,900
Open access books available

186,000
International authors and editors

200M
Downloads

154
Countries delivered to

Our authors are among the

TOP 1%
most cited scientists

12.2%
Contributors from top 500 universities

BOOK CITATION INDEX
CLARIVATE ANALYTICS
INDEXED

WEB OF SCIENCE™

Selection of our books indexed in the Book Citation Index
in Web of Science™ Core Collection (BKCI)

Interested in publishing with us?
Contact book.department@intechopen.com

Numbers displayed above are based on latest data collected.
For more information visit www.intechopen.com

Fluorescence Behavior of Phytoplankton Blooms by Time-Correlated Single-Photon Counting (TCSPC)

Helena C. Vasconcelos, Joao A. Lopes, Maria João Pereira and Afonso Silva Pinto

Abstract

Many aquatic ecosystems, such as lagoons or lakes, are increasingly vulnerable to climate changes and human pressure. The environmental and economic costs of anthropogenic eutrophication are high as well as the applied methods to counteract eutrophication This chapter analyzes the variation in abundance (and biomass) of several phytoplankton families in one of the most well-known volcanic lagoons in the Archipelago of the Azores-Portugal (Furnas Lagoon) and the dynamic correlation between groups of different types of algae that have been established seasonally between 2003 and 2018. For that purpose, the principal component analysis (PCA) technique was used in data series on biomass and abundance of phytoplankton and chlorophyll a, in the time interval considered. The application of PCA techniques in natural phytoplankton populations offers the possibility of making rapid qualitative diagnoses of the trophic state in natural lakes. On the other hand, the fluorescence properties of phytoplankton microorganisms are strongly affected by the physico-chemical properties of natural waters. The fluorescence emission and the lifetime of the different water samples were obtained by photon counting with time correlation (TCSPC), allowing to establish the fluorescent signature of these phytoplankton groups under certain conditions.

Keywords: Furnas Lake, Azores, phytoplankton, component principal analyses, fluorescence excitation, fluorescence lifetime, TCSPC

1. Introduction

The Azores archipelago is located in the North Atlantic Ocean (**Figure 1a**), limited by the parallels 36°55′43″ and 39°43′02″ N and by the meridians 24°46′15″ and 31°16′02″ W. The volcanic genesis of this archipelago explains the origin of many of its lakes and lagoons from volcanoes craters filled with rainwater. Although several of these bodies of water are now protected areas of high environmental value (e.g., Fogo, Sete Cidades, or Furnas Lake), some are undergoing trough an accelerated process of eutrophication (over enrichment with minerals and nutrients inducing an excessively growth of algae). The eutrophication of Furnas Lake (**Figure 1**), due to human agricultural activities, has been known since the 1980s and frequently
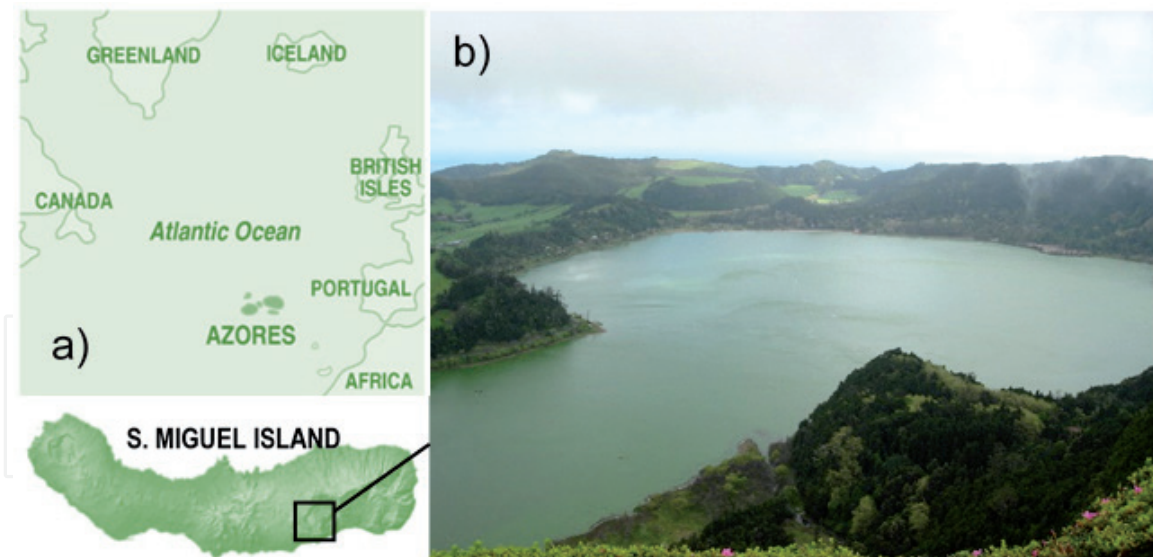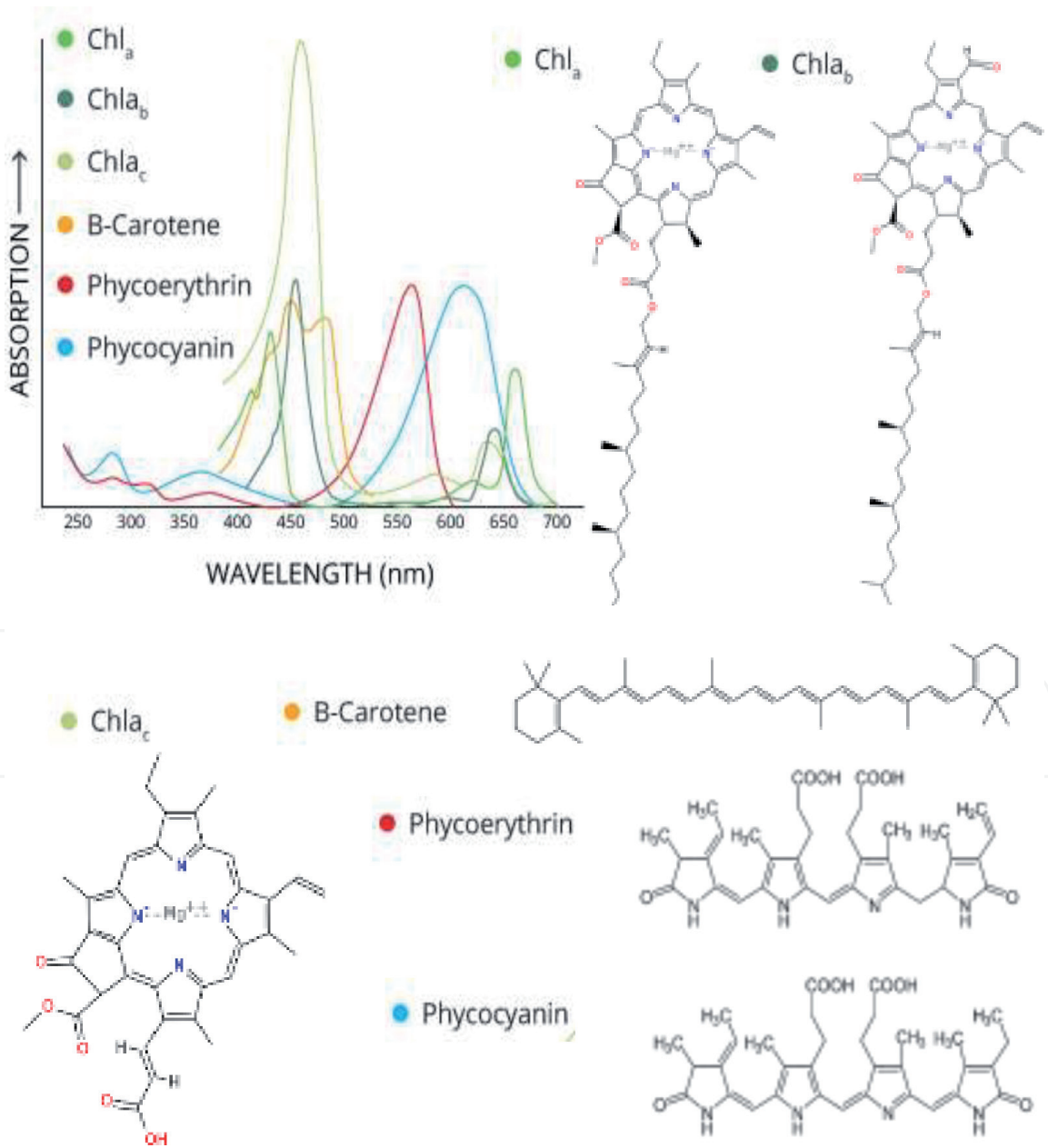
Figure 1.
(a) Azores archipelago localization, adapted from https://sunflowerbooks.co.uk/product/walking-in-the-azores/; (b) Furnas Lake, located in the eastern region of S. Miguel Island.

monitored afterward. The presence and extent of agricultural and forest areas in its basin allowed the drainage of nutrients to Furnas Lake causing algal blooms [1]. Eutrophication due to human activities is considered water pollution, and the phytoplankton community is currently used as a bio-indicator reflecting the lakes ecological state. The growth of phytoplankton often causes increased turbidity of the water, making difficult for sunlight to reach submerged plants. The disappearance of underwater vegetation implies the loss of food, habitats, and dissolved oxygen in water, distressing the trophic state of the ecosystem. Some types of algae can also produce toxins that are harmful vertebrates. Therefore, algae blooms disrupt the normal ecosystem functioning and causing problems along the food chain. The phytoplankton indicators highlight the vulnerability of these ecosystems to human activities since phytoplankton communities present high sensitivity to small changes in environmental conditions. The dynamics of phytoplankton biomass and composition over time reflects changes in environmental conditions. The aquatic ecosystems' degradation is associated with the increase of phytoplankton biomass—the "*blooms*"—a term used to mean a population concentration greater than 20×10^3 ml^{-1} [2]. This phenomenon, in particular in Furnas Lake, has occurred more frequently in the last years due to increase of human pressure [3].

Phytoplankton corresponds to the autotrophic organisms of the plankton community that are suspended in the water column. Phytoplankton includes a set of microalgae and cyanobacteria that have different requirements and responses to environmental variations. They have several photosynthetic pigments, such as chlorophylls (a, b, c, d and f), carotenoids (carotenes and xanthophylls), and phycobiliproteins. Chlorophyll a is, however, the key photosynthetic component, that is necessary in order for chloroplasts to convert light energy into chemical energy. The remaining chlorophylls, carotenoids, and phycobiliproteins (phycoerythrin and phycocyanin) act as accessory pigments in photosynthesis, expanding the range of light wavelengths that can be used in photosynthesis (e.g., chlorophylls d and f) [4] or protecting the photosystems against excessive light (e.g., carotenoids) [5]. Therefore, one can take advantage of the spectral optical properties inherent to the photosynthetic pigments of phytoplankton species, such as absorption and fluorescence, to obtain information about their characteristics by "spectral sets," that can be used to estimate, for instance, the phytoplankton biomass or composition in

lakes, reservoirs, or aquaculture [6, 7]. With the exception of chlorophylls *d* and *f* that absorb in far-red light [4], the chlorophylls absorb wavelengths in the visible blue and red spectrum, but not in the green spectrum. Chlorophyll makes plants and algae appear green because it reflects the green wavelengths, while absorbing all other colors. The different forms (*a*, *b*, and *c*) each reflects slightly different ranges of green wavelengths. The remaining pigments absorb different wavelengths (**Figure 2**) and reflect accordingly, but they all act as accessory pigments for chlorophyll *a* in photosynthesis. Carotenoids, for instance, absorb in the blue/green wavelength region and reflect yellow, red, and orange wavelengths.

Each type of pigment or sets of accessory pigments can be identified by the specific wavelength pattern they absorb from visible light [8, 9]. This allows discriminate optical signals between species of phytoplankton. In non-stressful conditions, when accessory pigments absorb photons, they become excited and transfer their absorbed energy between them, establishing a sequence of biophysical events until

Figure 2.
Optical absorption spectra of photosynthetic pigments. Adapted from https://www.fondriest.com/ environmental-measurements/parameters/water-quality/algae-phytoplankton-chlorophyll/.

reaching the chlorophyll a pigment (terminal of the excitation transfer channel), which emit fluorescence [10]. Chlorophylls will cause two main peaks in absorption spectra, a primary peak at blue wavelength (~440 nm) and a secondary peak in red part of the spectra (~675 nm) (**Figure 3**). The existence of other pigments (dependent on species and taxa) will cause the broadening of blue peak and appearance of additional absorption maxima. These taxa absorption peaks have been used as an optical spectroscopy tool in situ [11].

All photosynthetic plants, algae, and cyanobacteria contain chlorophyll *a*, while only green plants and green algae phytoplankton contain chlorophyll b, along with a few types of cyanobacteria in fresh water. The predominant forms of phytoplankton are diatoms, golden brown algae, green algae, blue green algae, and dinoflagellates. The taxonomy of phytoplankton is complex, and there are differences in classification systems. However, the classification currently followed in the study of phytoplankton in the Azores lakes comprises seven groups of phytoplankton *taxa* [14]: *Cyanophyta* (blue-green algae or cyanobacteria), *Chlorophyta* (chlorophytes or green algae), *Euglenophyta* (euglenoids), *Dinophyta* (dinoflagellates), *Cryptophyta* (cryptomonads), *Chrysophyta* (golden algae), and *Bacillariophyta* (diatoms). The blue-green algae, despite not having chloroplasts, have photosynthetic pigments, chlorophyll a and phycobiliproteins, which give them a predominantly blue color.

Eutrophication was recognized as a water pollution problem in European and North American lakes and reservoirs in the mid-twentieth century [15]. Since then, many efforts have been done to develop and apply appropriate mitigation methods and strategies [16]. The most usual procedure to study phytoplankton in water samples involves microscopic observation of the samples collected, thereby generating variable data that need to be careful processed (taxonomic technique).

A spectroscopic technique proposed in the 1980s [16] uses the excitation and emission characteristics associated with the fluorescence of the various photosynthetic pigments, to produce the fluorescence spectral signatures of specific water bodies. This allows the monitorization and detection of possible changes, due to environmental characteristics variation that can have impact on the relative
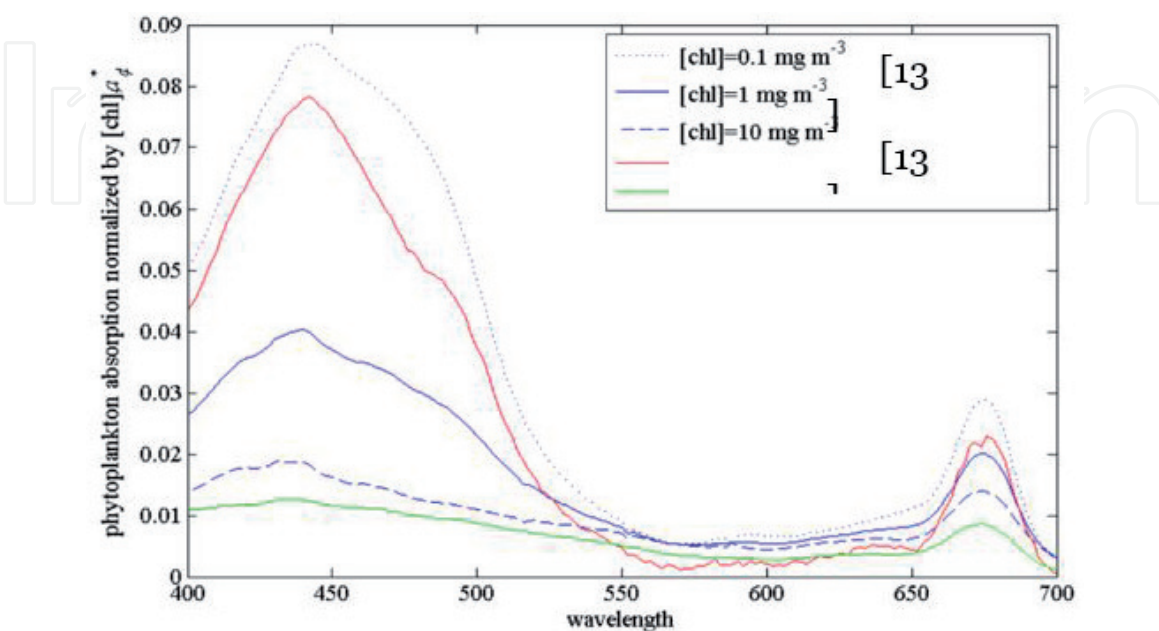
Figure 3.
Chlorophyll normalized phytoplankton absorption [12, 13]. Adapted from https://oceanopticsbook.info/index. php/view/optical-constituents-of-the-ocean/phytoplankton.

growth of phytoplankton populations. Since chlorophyll *a* and various pigments exhibit fluorescence in vivo and the qualitative and quantitative composition of phytoplankton pigments varies between taxonomic groups, its fluorescence properties also vary between taxonomic groups. Therefore, this tool can be used to discriminate changes in different *taxa* abundance [17, 18]. For example, diatoms and dinoflagellates exhibit typically broader excitation spectra than green algae and euglenoids. In cyanobacteria, the emission due to phycoerythrin is superior to the emission due to chlorophyll *a*, which is very much reduced. This main difference in the emission spectra usually makes cryptomonads and cyanobacteria easily separable from other types of phytoplankton, while differences in the excitation spectra can be used to separate green algae from diatoms and dinoflagellates [16]. Previous work has shown the effectiveness of fluorescence measurements in the characterization and discrimination of "spectral sets" of phytoplankton [8].

Differences in the spectral signature of some algal groups which differed in their pigment types are shown in **Figure 4** [19].

The measurements and interpretation of in vivo fluorescence signals from phytoplankton pigments can be affected by several sources, e.g., the algal physiology, the light conditions (quenching of fluorescence at high light intensity), the biomass concentration, and the differences in pigment composition between and within species [20]. Generally, factors such as environmental pollution and excess of nutrients alter the phytoplankton dynamics and consequently the rate of photosynthesis, which is revealed in the amount of fluorescence.

In this work, a rapid qualitative diagnosis of the trophic state of Furnas Lake was carried out. Associations established between the various phytoplankton communities (groups of taxa) over time have been identified using principal component analysis (PCA) [21]. In particular, the period from 2010 to 2011 was evaluated, looking for the most frequent taxa correlations in the different seasons. Additionally, the fluorescence spectra of some of these phytoplankton communities were obtained, as well as the lifetime of the fluorescence decays, using the time-correlated single-photon counting technique (TCSPC) [22].

The aim of this study was to use the potential of TCSPC for the rapid characterization of associated taxa in phytoplankton communities in vivo: (1) reveal the spectral signature and excitation/emission fluorescence spectrum associated with these communities and (2) their fluorescence lifetimes.
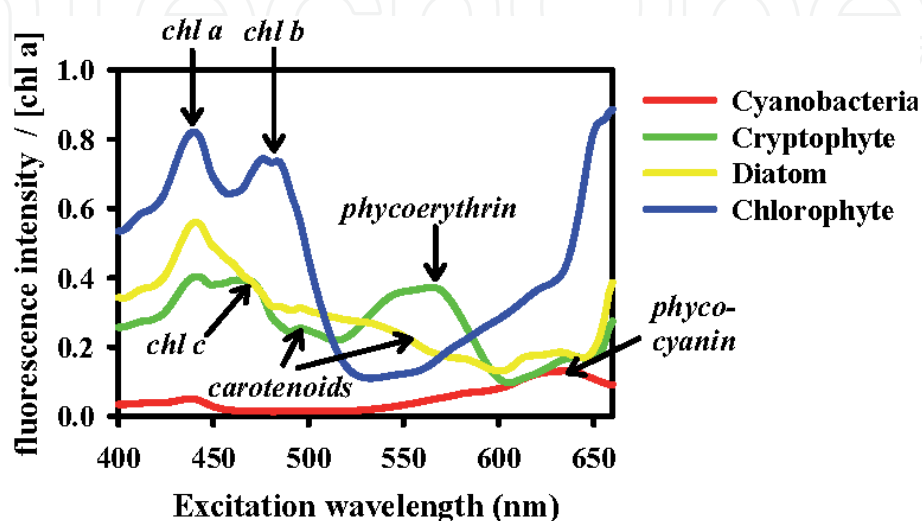
Figure 4.
Excitation spectra of some phytoplankton species measured at the maximum emission of chlorophyll a (682 nm) [19].

2. General overview about spectroscopy and fluorescence

Spectroscopy is the study of the interaction of electromagnetic radiation with matter. The natural world is filled with several colors that derive from the interaction process between matter and the visible radiation. The origins of spectroscopy date back to the seventeenth century, to the Newton's sunlight prisms work and observations of the multicolored band of light that he called spectrum. Since then, the terms "spectrum" and "spectroscopy" have been generalized in experiments of light scattered and decomposed into its different components.

Towards the end of the 19th century, J. Balmer discovery the spectral series of the hydrogen atom (1885), which allowed to determine the length of the hydrogen spectral lines. It was the discrete nature of atomic spectra that led to the formulation of some of the fundamental principles of quantum mechanics and, subsequently, their ability to explain spectroscopic observations.

The interaction of radiation with the matter can be manifested through absorption, emission, or scattering phenomena and be evaluated by spectroscopic methods. These are framed in the physical techniques of structural characterization of materials and are typically based on the absorption or emission of radiation with certain wavelengths (and photon energies), originating transitions between quantized levels. The results (optical spectra) are a representation of intensities as a function of wavelengths. Spectroscopy techniques are therefore methods that use radiation to analyze material properties and can be classified according to the type of transition they produce (**Table 1**). The response of matter to changes of incident radiation that falls within the range of 200 nm (UV) to 3000 nm (NIR) is generally evaluated by optical spectroscopy (UV-VIS-NIR regions). Photons emitted or absorbed when such changes occur are responsible for a large number of physical and chemical properties of matter. Electromagnetic radiation, commonly called light, is represented by electromagnetic waves characterized by a frequency (ν) and a wavelength (λ), related by the equation $\lambda\nu = c$, where c is the speed of light for a given medium. However, light also has particle properties (photons) with well-defined energy $E = h\nu$, where h is the Planck constant. Therefore, the light of wavelength λ is made up of photons with energy $E = h c/\lambda$.

Many of the physical-chemical processes that take place at the microscopic level are only explained on the basis of quantum mechanics. In particular, the concepts of quantified states of matter (Planck, 1900) and the nature of light (Einstein, 1905) describe how atoms interact with light and how electrons and energy levels within atoms are responsible for the absorption and light-emitting properties.

Transitions types	Techniques
Nuclear	Mössbauer spectroscopy
Electronic	Ultraviolet-Visible Spectroscopy (UV-Vis-NIR), ultraviolet photoelectron spectroscopy (UPS), and X-ray photoelectron spectroscopy (XPS)
Vibrational	Fourier-transform infrared spectroscopy (FTIR) and Raman
Rotational	Microwave rotational spectroscopy
Magnetic	Nuclear magnetic resonance (NMR) and electron paramagnetic resonance (EPR)

Table 1.
Spectroscopy techniques.

The main energy levels can only assume discrete values and is allowed only specific spatial distributions of electrons (called electronic energy levels); these levels are broken down into vibrational levels, which indicate the possible modes of vibration of the molecules. The first energy level (closest to the nucleus) is called the fundamental state (or ground state), and in it, the energies (electronic and vibrational) exhibit the minimum values. The other energy states of the molecule are called excited states.

It is easily to shown experimentally that a beam of electromagnetic radiation undergoes attenuation (intensity change, dI) when passes through an infinitely small part of matter (dx), following the Beer-Lambert law, which relates the absorption of light with the properties of the material crossed:

$$dI = -\alpha I dx \tag{1}$$

where I represents the light intensity and x the beam displacement.

$$\frac{dI}{I} = -\alpha dx \rightarrow \int_{I_o}^{I} \frac{dI}{I} = -\int_{o}^{x} dx \tag{2}$$

$$\ln \frac{I}{I_o} = -\alpha x \rightarrow I(x) = I_o e^{-\alpha x} \tag{3}$$

where I_0 is the radiation intensity and α is the absorption coefficient (cm^{-1}), which is a characteristic of each material. The transmittance (T) of a sample with a thickness d is defined as:

$$T = \frac{I}{I_o} = e^{-\alpha d} \tag{4}$$

The absorption cross section σ (cm^2) is defined as follows:

$$\sigma = \frac{\alpha}{N} \tag{5}$$

where N represents the concentration of absorbent centers (per cm^3), and σ is related to the capacity of the material to absorb the radiation at a specific wavelength λ.

Physically the photons absorbed by the electronic structure raise the energy of the molecule's electrons to quantum states less stable (excited).
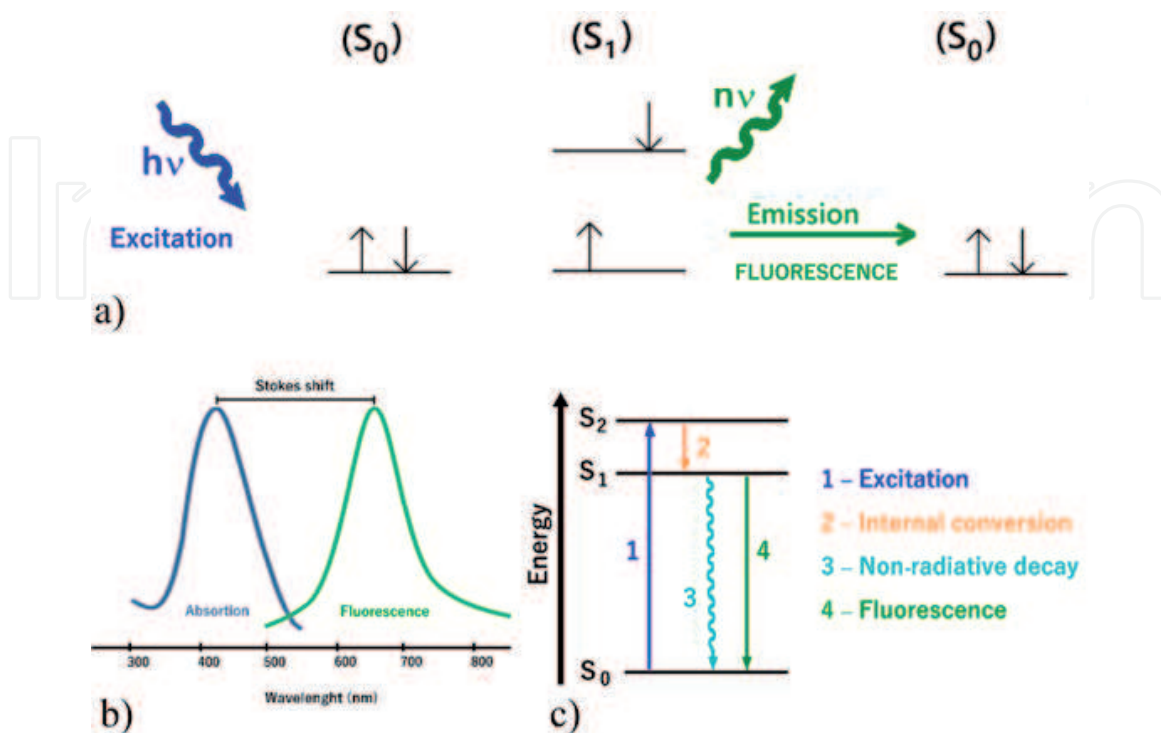
2.1 Fluorescence emission

The luminescence can be view like the reverse of the absorption process. If the material absorbs radiation and, consequently, is excited, it can then return to its ground state by spontaneous emission of light; this process of de-excitation is known as luminescence. The phenomenon is called fluorescence if this emission of light (emission of a photon) occurs quickly from a singlet excited state, in which the

excited electron does not change the spin orientation and remains unpaired, which allows its return to the fundamental state. The typical fluorescence lifetime is in the order of 10^{-9} s, which corresponds to a fluorescence emission rate $\sim 10^8$ s^{-1} [23, 24]. A fluorescence emission spectrum is a curve of fluorescence intensity (I) versus wavelength (λ).

Basically, a photon of appropriate energy is able to excite an electronic transition in which an electron from the singlet state S_0 passes to a higher energy level of S_1 (**Figure 5a**). This excitation (absorption of a photon of light) occurs instantly (femtoseconds). Once the material is excited at a wavelength where it absorbs, the system can return to its ground state. Fluorescence is a radiative mechanism by which excited electrons can relax in a fast process (nanoseconds), by emitting light from the lowest excited state (S1) to the ground state (S0). The energy difference between the two states is dissipated by emitting a photon.

An interesting detail is that the emitted light has a longer wavelength than that of absorption radiation (excitation) (effect named Stokes Shift), as shown in **Figure 5b**. This is due mostly because the energy loss during the electronic excitation is also due to transition of electrons to lower vibrational levels, caused by release of thermal energy due to internal conversions, named as non-radiative decay. The fluorescence is therefore independent of the emission wavelength from the excitation wavelength (Kasha's rule), i.e., the fluorescence emission will always originate from the vibrational ground state of the lowest excited singlet level, S1. Even if the electron is excited to higher vibrational levels of S1, it mainly undergoes relaxation from S1 to S0. **Figure 5c** shows a simplified Jablonski diagram, which illustrates the energy states of a molecule and the transitions between them. Transitions between states are represented by vertical lines in order to show the instantaneous nature of light absorption. The times for the occurrence of the transitions are in fact very short, in the order of 10^{-15} s, which does not allow displacements of the nucleus (mass greater than that of electron), a fact known as the Franck-Condon principle [23]. To achieve stability, the molecule dissipates the

Figure 5.
(a) Excitation and fluorescence emission after absorption of light; (b) Stokes shift; and (c) Jablonski diagram (simplified).

energy absorbed by radiative and/or non-radiative decay processes (**Figure 1c**). The radiative decay processes involve the emission of photons, and this emission can occur by fluorescence in a time range of the order of nanoseconds of lifetime τ, typically less than 10^{-8} s [23]. The non-radiative processes occur by internal conversion, due to vibrations and rotations of the molecule or, in some cases, by energy transfer to neighboring molecules through collisions.

Transitions between states are represented by vertical lines in order to show the instantaneous nature of light absorption. The times for the occurrence of the transitions are in fact very short, in the order of 10^{-15} s, which does not allow displacements of the nucleus (mass greater than that of electron), a fact known as the Franck-Condon principle. At room temperature, thermal energy (E ~ KT) is not sufficient to cause a significant population of excited vibrational states. Photon absorption occurs in functional groups of molecules with lower vibrational energy, and the fluorophore is excited to some higher vibrational level of its S1 singlet states.

2.2 Fluorescence lifetime and quantum yield

The fluorescence lifetime of a substance generally represents an average value of time that a molecule remains in the excited state before returning to the ground state. The characteristics of the fluorescent decay can reveal details about the interactions of fluorophores with its neighborhood. The fluorescence decay time is sensitive and can be affected by local molecular surroundings, which may cause changes in decay time [23, 25–27].

This technique reveals the change of fluorescence intensity as a function of time after the establishment of the excited state. It displays the evolution of the excited state reactions and the mechanism by which they return back to the ground state. Measurements of fluorescent lifetime are difficult as these times are typically in the nanosecond range, making it necessary to use high-speed electronic devices and suitable detectors. The excitation of a fluorophore with an ultra-short pulse of light, at time $t = 0$, results in an initial population (N_0) of fluorophores in the excited S1 singlet state through the absorption of photons. The excited molecules can decay to ground state by radiative or non-radiative processes giving a signal of intensity decay. The rate of change of the population of excited states, $N(t)$, after instantaneous pulse excitation, follows the equation:

$$\frac{dN(t)}{dt} = -W_T N(t) \tag{6}$$

where the total decay rate constant, W_T, is the sum of the rate constants for all radiative (R) and non-radiative (NR) decay processes ($W_T = W_R + W_{NR}$). Following integration of Eq. (6), the concentration of the excited states $N(t)$ is given by the following equation:

$$N(t) = N_o e^{-W_T t} \tag{7}$$

where N_0 is the density of excited electrons at t = 0 just after the pulse excitation be absorbed. The de-excitation process can be observed experimentally by analyzing the lifetime decay of the emitted light (fluorescence decay) (**Figure 6**). The parameter monitored during fluorescence lifetime experiments is the fluorescence
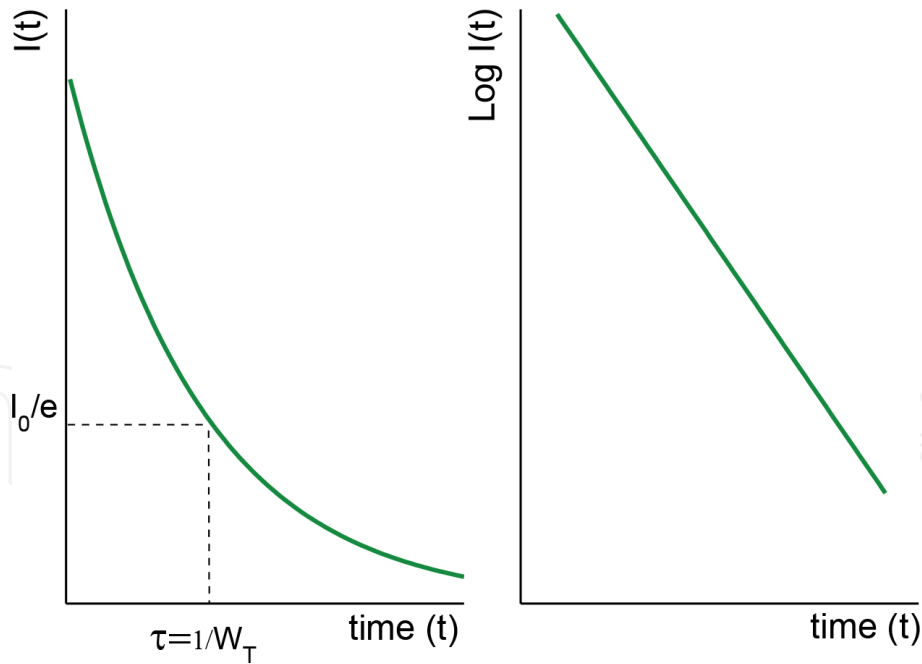
Figure 6.
Scheme of a fluorescence decay curve using pulse method. Adapted from Ref. [23].

intensity, $I(t)$, which is the rate of the emission of photons and is related to the excited state concentration by the following equation:

$$I(t) = W_R N(t) = I_o e^{-W_T t} \qquad (8)$$

where $I_0 = W_R N_0$ is the intensity at $t = 0$.

Therefore, the intensity decays exponentially after the initial excitation pulse. The fluorescence lifetime of the excited state, τ, can be represented as $\tau = (1/W_T)$. The fluorescence lifetime represents the time in which the emitted intensity decays to 1/e of that initially excited and gives us the total rate of decay (radiative + non-radiative); therefore, τ is given by the following equation:

$$\frac{1}{\tau} = \frac{1}{\tau_o} + W_{NR} \text{ and } \frac{1}{\tau_o} = W_R \qquad (9)$$

where τ_0 is the radiative lifetime. Fluorescence quantum yield, η, can be obtained through the Eq. (10), in terms of τ_0 and τ, as follows:

$$\eta = \frac{W_R}{W_R + W_{NR}} = \frac{\tau}{\tau_o} \qquad (10)$$

Briefly, η is defined as the ratio between the radiative decay rate and the total decay rate. The total decay rate can be obtained experimentally as the inverse of the lifetime decay of the emitted light (obtained in the laboratory), while the rate of radiative decay, usually more difficult to obtain, is the inverse of radiative lifetime. The lifetime can be influenced by quenchers, i.e., the process that leads to a decrease in fluorescence (quenching is a form of internal conversion) [23].

Quantum yield is a dimensionless gauge to assess the efficiency of fluorescence emission relative to all of the possible ways for relaxation and is expressed as the ratio of photons emitted to the number of photons absorbed. This means that the quantum yield corresponds to the probability that an excited molecule will produce an emitted photon (fluorescence). Quantum yields range between a value of 0 and 1.

The emission spectrum can be obtained at different times after the absorption of the excitation pulse; this experimental procedure is called luminescence resolved in time. The basic idea of this technique is to obtain the emission spectrum with a certain delay t, with respect to the excitation pulse within a time window Δt.

The lifetime can also be considered as the average value of the time that a fluorophore remains in the excited state. However, for very complex decay laws, such as multi-exponential or non-exponential decays, the adjustment is made by a sum of exponentials of the type [23]:

$$I(t) = \sum_i B_i e^{-\frac{t}{\tau_i}} \tag{11}$$

where τ_i is the lifetime of component i of the decay and B_i is the corresponding pre-exponential factor. Thus, the average lifetime is given by the following equation:

$$\tau_{av} = \frac{\sum_i B_i \tau_i^2}{\sum_i B_i \tau_i} \tag{12}$$

3. Methods

3.1 Study area

The Azores are an Archipelago of nine islands in the North Atlantic Ocean, from 37° to 40 N latitude and 25 to 31ºW 125 longitude. Its location coincides with the confluence of three tectonic plates which makes this archipelago a complex geodynamic system with a volcanic genesis [28].

The Furnas Lake is located on the island of São Miguel in a volcanic crater. The lake has an area of 1.87 km^2 and a maximum length and width equal to 2025 and 1600 m, respectively [29]. Agriculture and fertilized pastures are the most common activities in its hydrographic basin, contributing to the lake's nutrient load and causing increasing eutrophication. Over the past 20 years, a local meteorological station recorded average air temperatures in this region ranging from 11°C in winter to 20°C in summer (data provided by Azores Regional Environmental Office). The climatic characteristics in the region favor the occurrence of severe rains, and as a result, large amounts of nutrients are easily transported to the lake. Because the temperature in the S. Miguel island is adequate for phytoplankton growth throughout the year and the nutritional conditions favor cyanobacteria development [2], the lake has exhibited several episodes of algal blooms over time [30]. Although the lake is part of a protected landscape area, the economic activities that contribute

to local development often override environmental authorities, and the use of fertilization around the lake has facilitated the entry of nutrients. In 1988/89, the lake was classified as eutrophic (average Carlson's TSI for chlorophyll *a* was 66) [30]. Carlson's Trophic State Index (TSI) is a common method for characterizing a lake's trophic state. This method uses Secchi disc transparency, chlorophyll *a*, and phosphorus measurements.

Previously studies showed that the phytoplankton populations in Furnas Lake exhibited a high abundance divided into two main groups, diatoms and cyanobacteria. In spring, there is a very high relative abundance of Bacillariophyta (diatoms). In summer and autumn, there is a presence of persistent blooms of cyanobacteria, indicators of reduced biodiversity in the lake [3]. The bloom-forming cyanobacteria dominate the phytoplankton of the eutrophic Furnas Lake, as expected during the summer thermal stratification period [31].

In order to mitigate this problem, the Azores government has initiated several actions to counteract the Furnas Lake eutrophication [32–35].

3.2 Sampling and available data

The sampling collection took place between January and December 2011. **Table 2** exhibits the sampling conditions, and **Table 3** summarizes the labeling of samples and date of collection.

The used biological data [chlorophyll a and phaeopigments (μg/L), abundance (cell/L), and phytoplankton biomass (10^{-9} mg/L)] were obtained from the Azores Regional Government—Water Monitoring website [36] in the periods 2003–2018. The selected phytoplankton data totaled seven phyla (**Table 4**) and corresponded to the analysis of samples collected according to **Table 2**. For the assessment of trophic status, information on chlorophyll *a* concentration (an indicator of phytoplanktonic biomass) and phaeopigments were used.

The Matlab program, version R2016b (MathWorks, Natick, MA) was used to perform PLS Toolbox version 8.2.1 for Matlab (Eigenvector Research, Manson, WA) for the PCA analysis.

3.3 Time-correlated single-photon counting (TCSPC)

Fluorescence techniques are methods that exploit the phenomenon of fluorescence. They have been widely used in the characterization, in vivo, of phytoplankton communities of diverse aquatic ecosystems [6, 7]. These methods allow estimate the concentration of chlorophyll a (or other pigments) and the electron transfer rates during photosynthesis. The pigments whose function is to collect light and transfer the absorbed energy to the reaction centers (antenna pigments)

| Sampling type	Sampling equipment	Sampling technique	Laboratory method
Collection of water samples	"Van Dorn" water collection bottle	Each water sample was collected at various depth levels (surface, middle, and bottom) and the ultimate sample consisting of homogenization of identical volumes of water collected at each of the sampling depths	Phytoplankton samples were kept fresh and in the dark until analysis, which started in 24–48 h after collection, to minimize pigment degradation.

Table 2.
Sampling conditions.

Sample labeling	Date of collection
A1	2011, later spring (June)
A2	2011, winter (February)
A3	2011, early autumn (December)
A4	2011, spring (May)
A5	2011, summer (August)

Table 3.
Labeling of samples and date of collection.

Scope	Descriptors (variables)
Biological (phytoplankton phyla)	Cyanophyta (aka. Cyanobacteria), Chlorophyta, Euglenophyta, Dinophyta, Chrysophyta, Cryptophyta, and Bacillariophyta
Biological (trophic assessment)	Chlorophyll *a* and phaeopigments

Table 4.
Data groups and variables in each group.
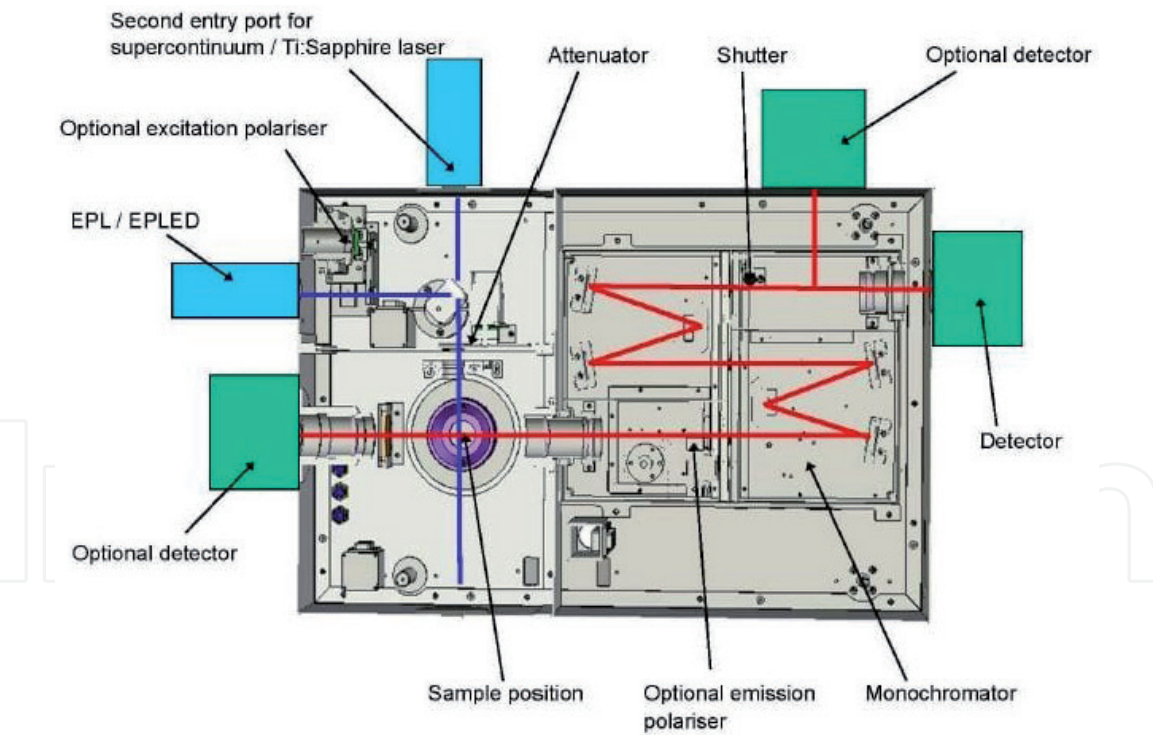
Figure 7.
*Layout of the Spectrofluorometer LifeSpec II [37] (optional and main components).*

vary between the phytoplankton taxa. Therefore, the characteristics of the phytoplankton in vivo fluorescence, including its fluorescence efficiency, depend on the taxonomy. Chlorophyll *a* fluorescence reflects the concentration of this endogenous pigment.

Fluorescence is a phenomenon that competes with the use of photons absorbed by the antenna pigments in photosynthesis. However, if the photon capture mechanism is necessary to perform photosynthesis changes, increasing

its efficiency or decreasing it, the fluorescence intensity [$I(t)$] will also be changed. Thereby, the main goal of measuring fluorescence decay profiles is to determine the $I(t)$ function. Typically, the decays observed are set to a sum of exponentials [23].

There are several commercial processes and instruments to induce the fluorescence of phytoplankton photosynthetic pigments in vivo. Since the fluorescence lifetime of the organic molecules is in the ns or ps order, it requires the use of high temporal resolution techniques and making use of excitation pulses to follow the pattern of fluorescent emissions over time. Time-correlated single-photon counting (TCSPC) spectroscopy is one of the most suitable techniques for allowing the measuring of shorter times and multi-exponential decay with great accuracy.

A spectrofluorometer of the type LifeSpec II from Edinburgh Instruments [37] was the instrument used in this work. The measurements were performed with a pulsed EPL-406 nm diode laser with 80 ps of pulse duration as the excitation source. All measurements were performed at room temperature. **Figure** 7 shows the layout of the measuring device.
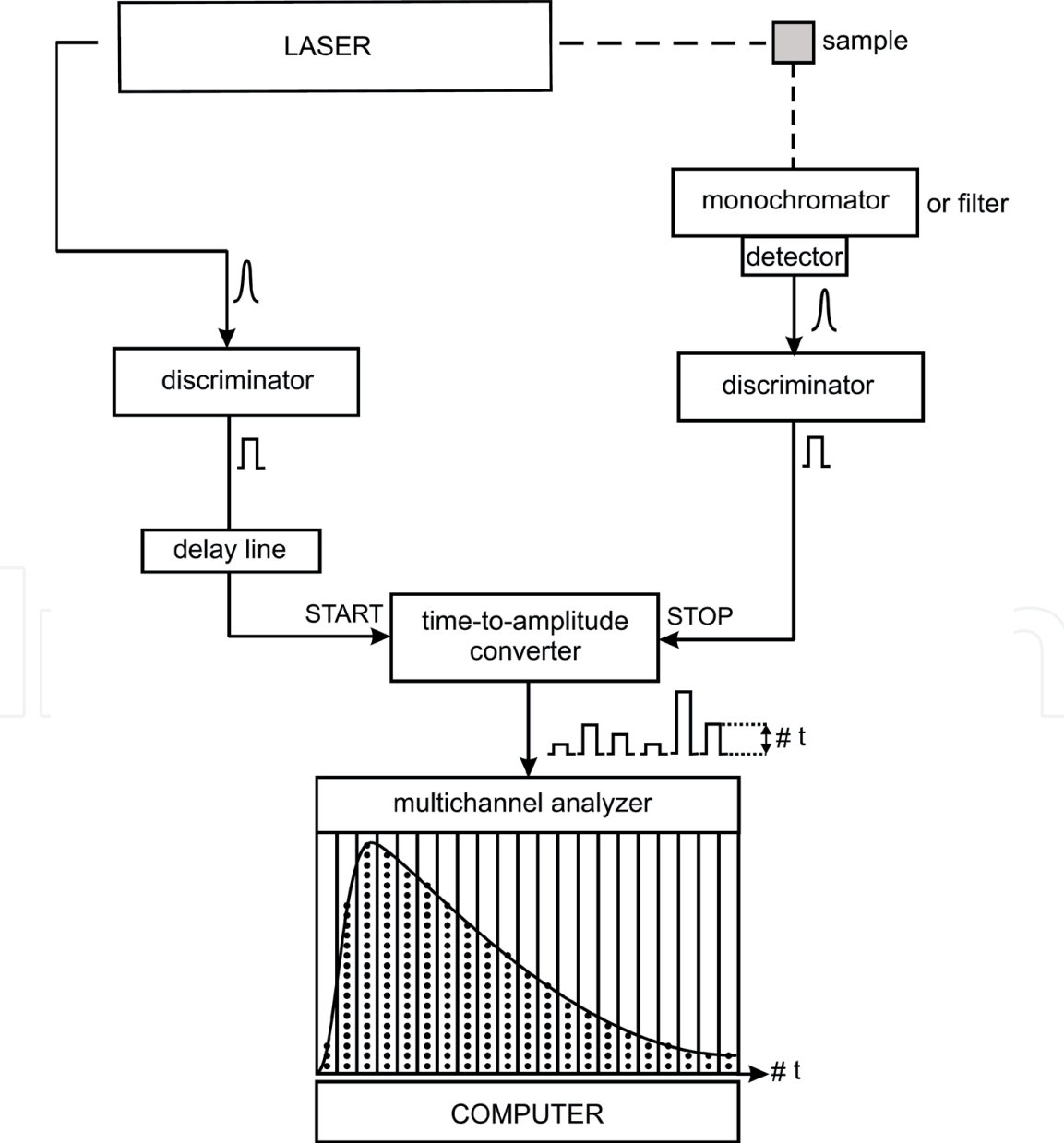
Figure 8.
TCSPC schematic layout. Adapted from Ref. [39].

The principle of TCSPC is the detection of single photons and the measurements of their arrival times with respect to the excitation light pulse [38]. TCSPC is a statistical method, and a repetitive light source is used to accumulate a sufficient number of photon events for a required statistical data precision.

Briefly, TCSPC measures the time delay between two signals, the signal of fluorescence that comes from the sample and the signal of an electrical pulse generator which triggers the laser source. After being triggered by the electrical pulse generator, the excitation laser produces pulsed light with the same time profile as the electrical pulse. These electrical pulses are guided, at the same time, to the laser and to the detector and that time is set as 0. Then, the detector compares the time delay between both signals, that which triggered the laser and that emitted from the sample, and then it sets a count corresponding to the exact time delay of the photon relative to the electrical pulse. TCSPC can be compared to a fast stopwatch with two inputs (**Figure 8**) [39]. The clock is started by the START signal pulse and stopped by the STOP signal pulse. The process is repeated several times and so more and more photons are added on the histogram. The resulting histogram counts versus channels will represent the fluorescence intensity versus time [38].

The term single-photon counting comes from the fact that in the pause between two consecutive excitations (or pulses), only one photon, emitted by the sample, can be detected. When this photon is detected, it added to the previous photons which had the same time delay on the histogram.

The emitted photons were collected at the maximum emission length of the studied samples. Before the sample measurements, the equipment's instrument response function (IRF) was measured. The IRF represents the shortest decay curve that can be measured with that equipment.

4. Results

4.1 Analysis of principal components (PCA)

Phytoplankton populations in the Azores lakes are represented by their most common phyla, namely, Bacillariophyta, Chlorophyte, Cryptophyta, Chrysophyta, Cyanophyta [aka cyanobacteria (Cyanoprokaryota)], Dinophyta (Pyrrophyta), and Euglenophyta [3]. The trophic state and composition of the phytoplankton community can be made through temporal (abundance and/or biomass) records and further analysis of patterns of variation of these communities by statistical techniques. A PCA of the phytoplankton data was performed, and two models were created considering the abundance data (measured in cells/L) and biomass data (measured in 10^{-9} mg/L).

4.1.1 Multivariate analysis of phytoplankton abundance

Figure 9 shows the correlations between the seven abundant phytoplankton phyla in Furnas Lake and identifies algal assemblages showing how these associations correlate with each other in the period 2003–2017.

The graph is analyzed as follows: the variables (descriptors) that are close to each other have a high positive correlation and the variables that are diagonally opposite are negatively correlated. For example, it seems that the Chlorophyta and Chrysophyta phyla appear very close, meaning that there is a high correlation between the abundance of these two phytoplankton phyla. On the fourth quadrant, we can see that Cyanophyta (Cyanoprokaryota) is inversely correlated with Bacillariophyta, while it exhibits more affinity with Pyrrophyta. On the other
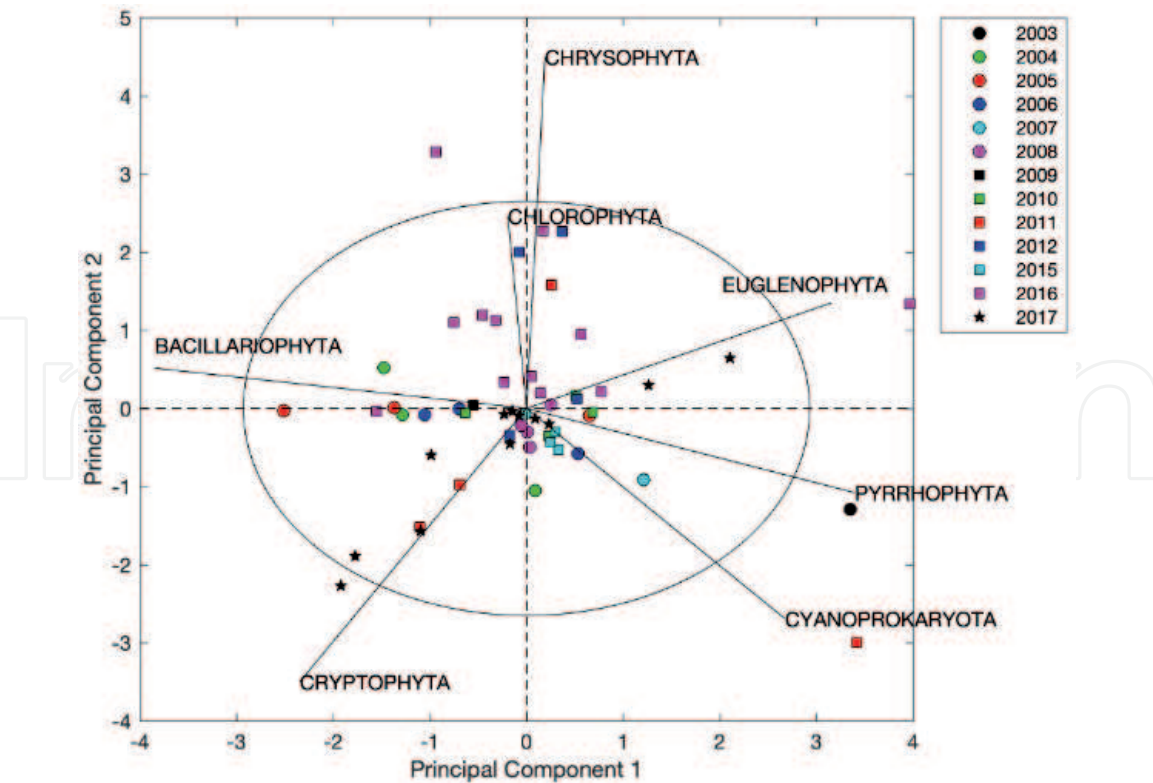
Figure 9.
Multivariate analysis (PCA) of abundance (cells/L) for phytoplankton descriptors (colored by year).
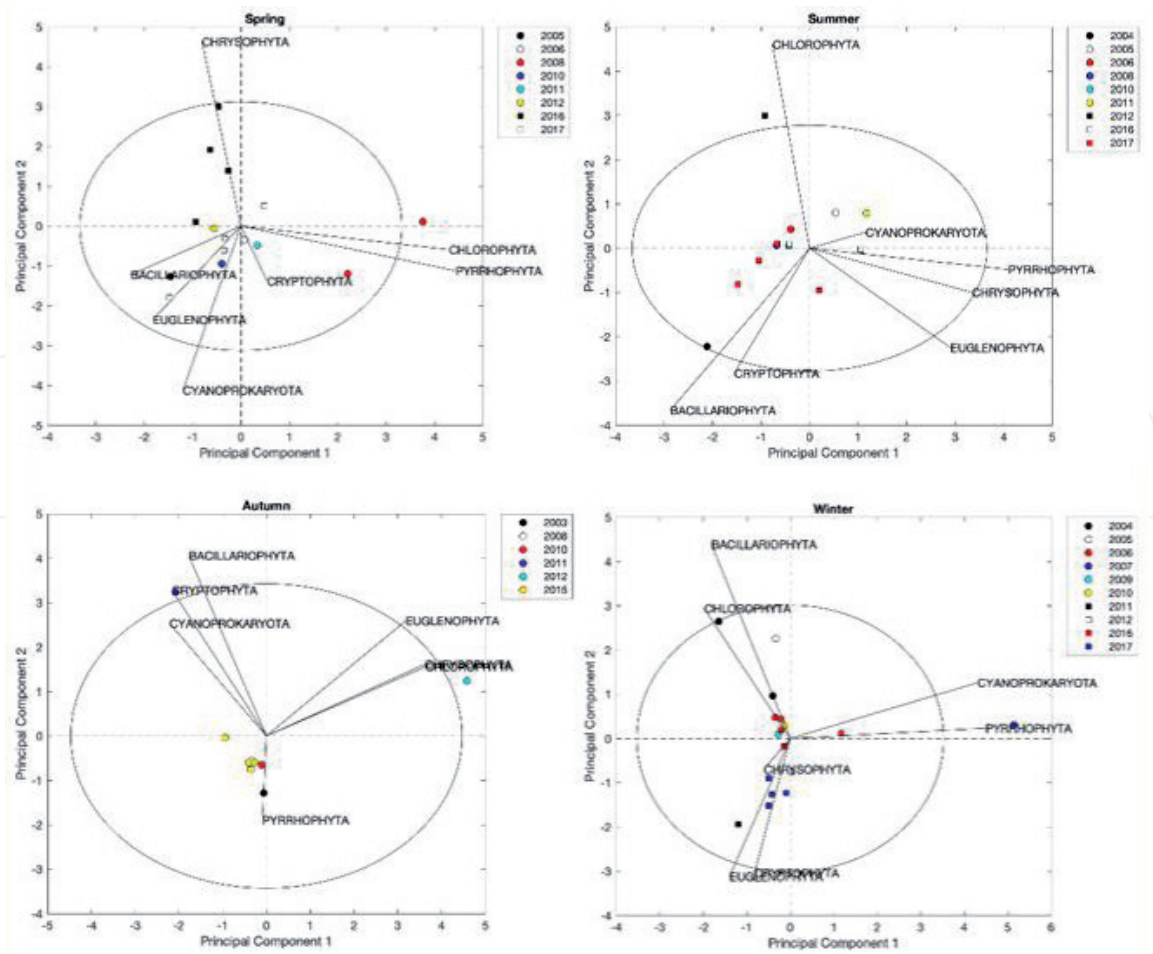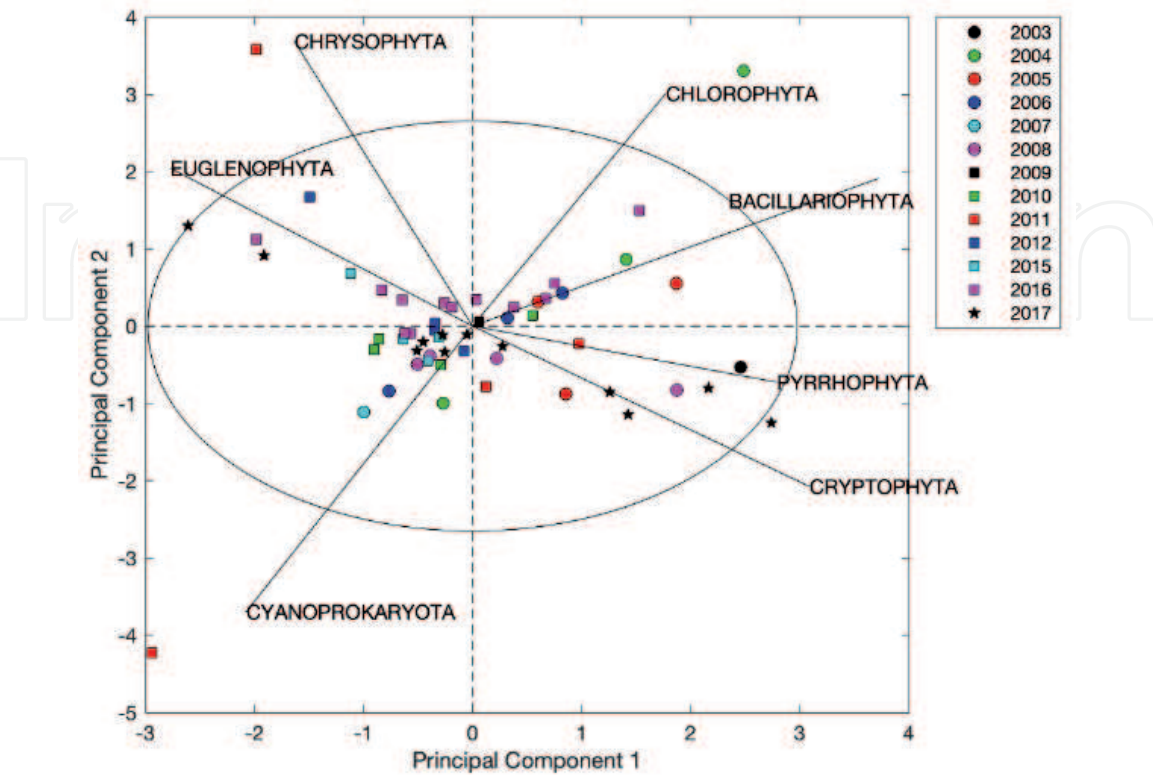

Figure 10.
Multivariate analysis (PCA) of abundance (cells/L) for phytoplankton descriptors, by seasons (colored by year).

hand, although most of the points are found to be located very close to the center without much year variability, some are distant, corresponding to situations where the abundance of phytoplankton phyla increases far beyond the limit of the corresponding circle at the confidence interval. For example, in 2011, it seems that a bloom of Cyanoprokaryota occurred, during which the abundance of these organisms reached maximum values. Records show that blooms have not occurred as pronounced since 2006–2007. Records also show that the abundance of Chlorophyta had a very significant increase in 2016 when it was practically non-existent in previous years. However, this situation can be considered sporadic, since in 2017 there was again a decrease.

Figure 10 exhibits the phytoplankton correlations throughout the seasons, where the high abundance is divided into two main groups, diatoms and cyanobacteria. In spring, there is a very high relative abundance along years of Bacillariophyta (diatoms). In summer, there is a presence of persistent blooms of cyanobacteria, indicators of reduced biodiversity in the lagoon [3]. The bloom-forming cyanobacteria dominate the phytoplankton of the eutrophic Furnas Lake, as expected during the summer thermal stratification period [31]. In particular, in 2011, the record shows that bloom-forming cyanobacteria reached a maximum value. In Furnas Lake, cyanobacteria often dominate the phytoplankton population in summer, early autumn and later spring, whereas during the winter and early spring, they are replaced mainly by Bacillariophyta and Chlorophyta. The data set considers summer from July to September and autumn from October to December.

4.1.2 Multivariate analysis of phytoplankton biomass

For biomass data (**Figure 11**), the analysis is relatively similar to that for abundance data, except that Chlorophyta appears to have a negative correlation with Cyanoprokaryota. Warming temperatures of the lakes since there is also
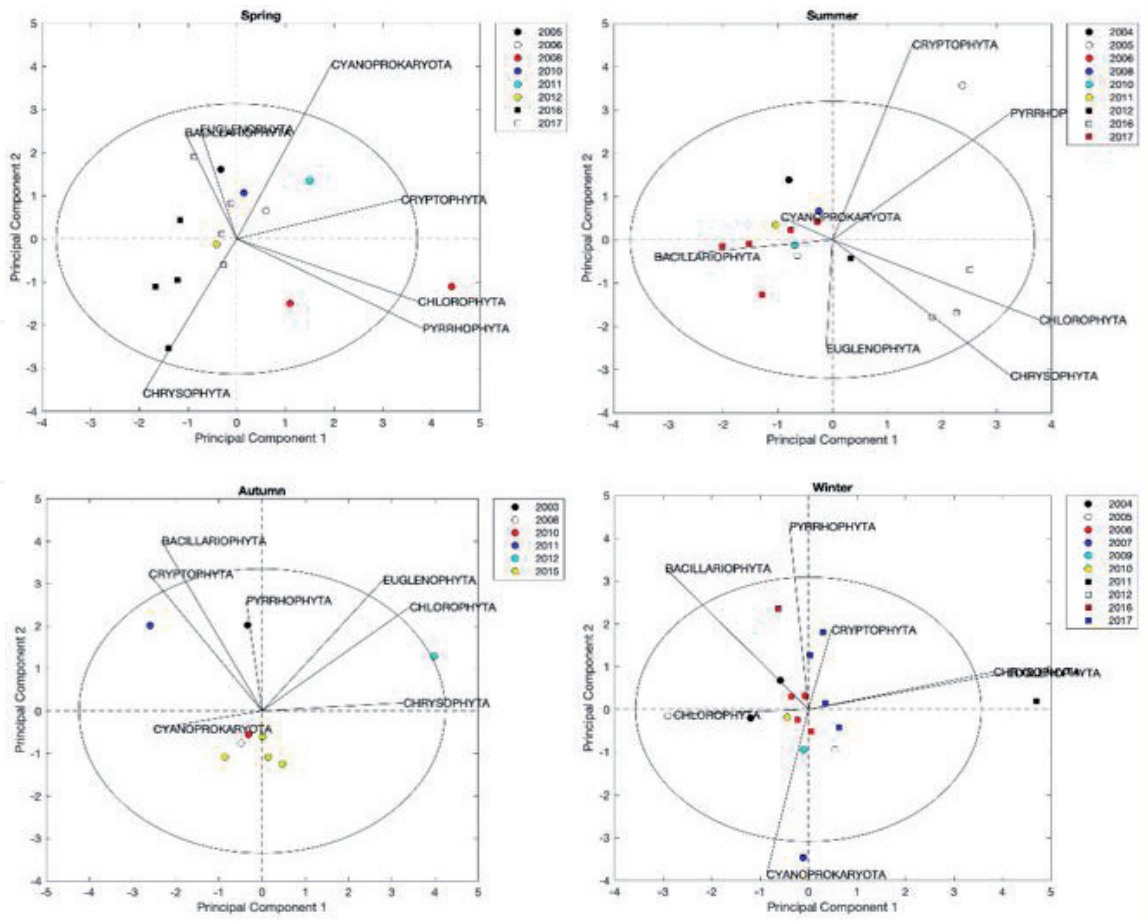

Figure 11.
Multivariate analysis (PCA) of biomass (10^{-9} mg/L) for phytoplankton descriptors (colored by year).

a correlation between the green algae and cyanobacteria with warmer seasons (summer), which leads to limited transport between layers causing a lake stratification.

The analysis of the results, although still preliminary, allows to some extent confirm that the phytoplankton composition in the lake of Furnas reflects its trophic status, which is obviously higher (i.e., of low water quality) when is found a predominance of Cyanoprokaryota, while a lower trophic state (oligotrophic or mesotrophic) seems to be related to the presence of Chlorophyta and also Bacillariophyta. Moreover, Chlorophyta is negatively correlated with Cyanoprokaryota, especially in summer, but correlated positively with Bacillariophyta, suggesting competition between these two groups (**Figure 12**) [40].

Chlorophyta can also be predominant in lakes with high concentrations of phosphorus [41], such as the lake of Furnas, and may change with the dynamics of the eutrophication state [42]. It is therefore probable that competitive interactions between Chlorophyta, Cyanoprokaryota, and Bacillariophyta can occur under nitrogen and phosphorous gradients [40].

Since 2002, Lake Furnas shows a constant state of eutrophication [3], with average annual values of the trophic state index based on Secchi disk between 57 and 70, characteristic of eutrophic media, and average annual values of the trophic state index based on phosphorus total between 45 and 67, characteristic of mesotrophic and eutrophic media. The value 45, obtained from this last index, allowed a mesotrophic classification in 2014. Between 2013 and 2016, the annual values of the TSI corresponding to chlorophyll varied between 54 and 55, characteristic of eutrophication [3].

Figure 12.
Multivariate analysis (PCA) of biomass (10^{-9} mg/L) for phytoplankton descriptors, by seasons (colored by year).

4.1.3 Multivariate analysis of chlorophyll a and phaeopigments

Concerning the analysis of chlorophyll *a* and phaeopigments, the results are recorded in the scores of **Figure 13**. The chlorophyll *a* degradation products can often form a significant fraction of phaeopigments, which correspond to byproducts formed by the loss of Mg atom (**Figure 2**), generally under acidic conditions [43]. As phaeopigments may originate from chlorophyll *a*, some correlation between these two descriptors was expected. Taking into account the apparent occurrence of a bloom of Cyanoprokaryota in 2011, a more detailed analysis of these two descriptors was conducted between 2010 and 2011.

The multivariate analysis of the concentrations of chlorophyll a and phaeopigments reveal an expected positive correlation and some patterns that are worth to discuss. This correlation is stable over time. The analysis segregated by year reveals different tendencies of abundance. While in 2010 and 2012, the abundance of both indicators is higher in autumn and winter, especially in winter. This trend was not observed in 2011 where the concentrations were higher in spring and summer. It is noteworthy to say that this analysis was based on a relatively short dataset encompassing approximately three observations per season.

A global analysis to these data considering years from 2003 to 2018 reveal some prevalence patterns (**Figure 14**). While the correlation between the two indicators stays relatively stable over time, it can be observed a high concentration of chlorophyll *a* in water in 2004 and 2009 (eventually one can include here also 2005 and 2006 at least in some periods of the year). Concerning the levels of phaeopigments, there is a clear evidence of the gradual increase starting in 2011. It is clear the increasing occurrence of phaeopigments after 2011 that was still observable in 2018. For some years (e.g., 2016), it was found that simultaneously with a high occurrence of phaeopigments in some periods of the year, there is also an observation of very low amounts in other periods of the year, widening the range of concentration observed in a single year.

The seasonal variation is controlled mainly by solar radiation and temperature, which will determine the stratification of the water column and the availability of nutrients.

4.2 Fluorescence behavior

Phytoplankton organisms have a wide range of photosynthetic pigments that are of great interest in identifying species in freshwater samples representing different phytoplankton communities [11]. Although microscopy is a method widely used to determine the structure of the phytoplankton community, it is an exhausting and time-consuming process. Hence, the great interest is in fluorescence studies of these communities, using the knowledge of the specific excitation bands of the photosynthetic pigments, in order to have access to the probable types of phytoplankton communities. But for this task, it is necessary to know that there are two main regions of excitation of phytoplankton pigments: the blue (400–520 nm) and red (630–700 nm) regions, which can be seen in **Figure 4**. In the green (515–600 nm) region, there are some absorption bands attributed to phycobilins. Fluorescent spectroscopy began to be used extensively in the characterization of phytoplankton taxa from the 1980s, particularly after the development of an "ataxonomic tool" [16]. In vivo fluorescence methods are widely used to characterize phytoplankton communities, but the taxonomic identification of algae taxa is still a challenge. Measurements of the fluorescence intensity of phytoplankton communities are affected by varying concentrations of biomass, and therefore, a variable contribution to the fluorescence signal can be expected in different subpopulations, as well
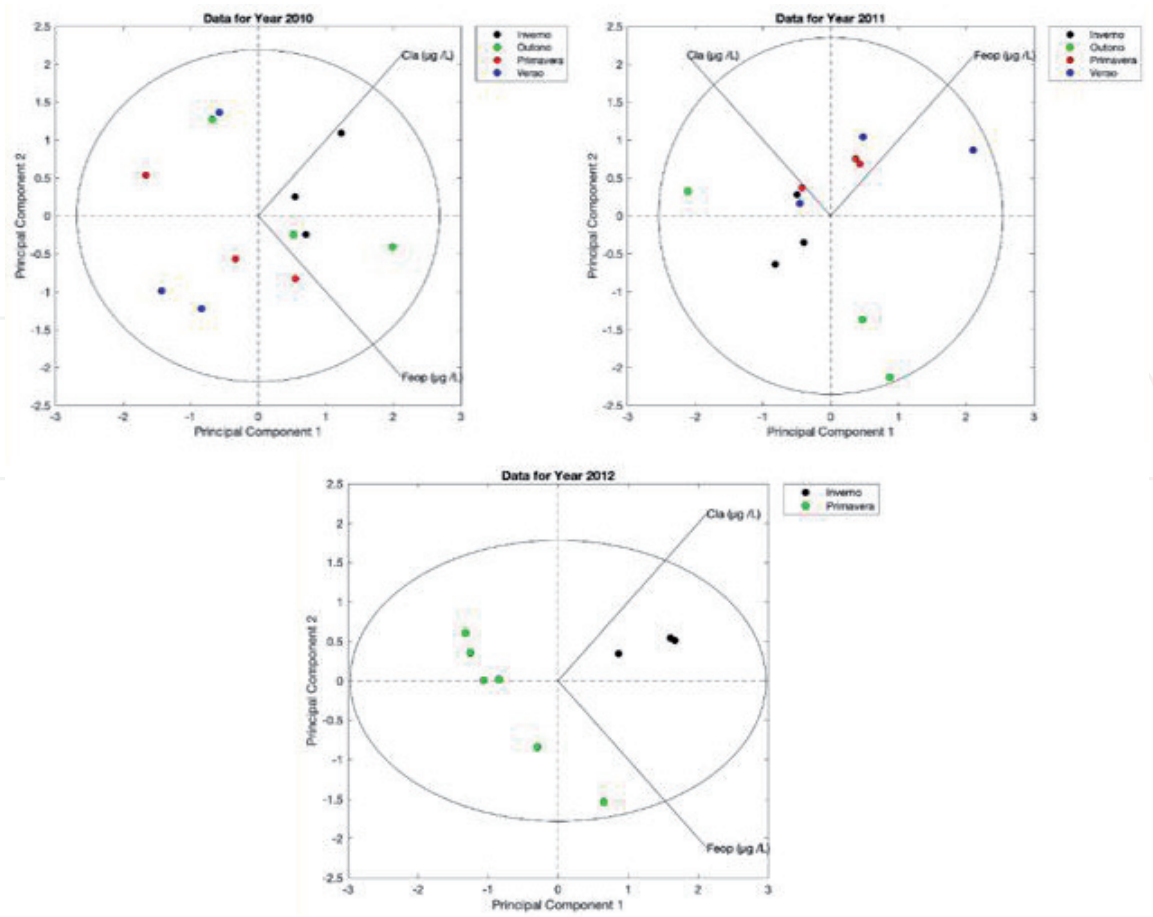
Figure 13.
Multivariate analysis (PCA) of chlorophyll a and phaeopigments (2010–2012, colored according to season).
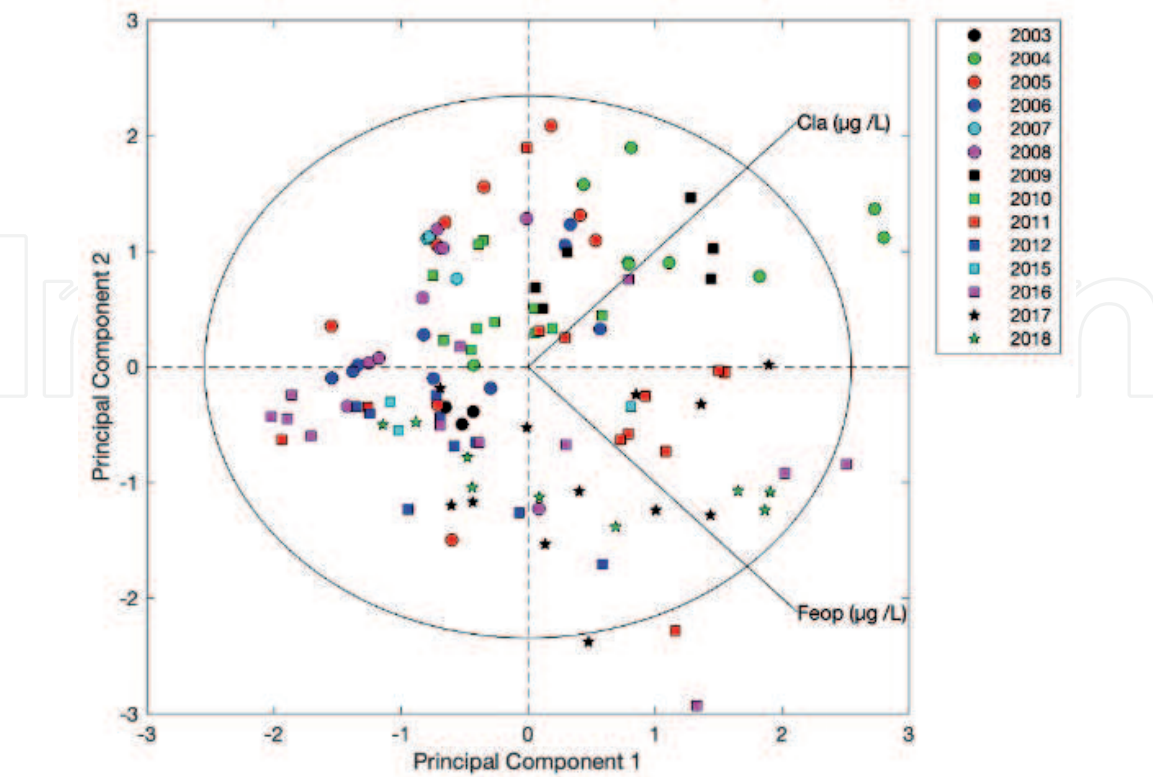
Figure 14.
Multivariate analysis (PCA) of chlorophyll a and phaeopigments (colored according by year).

as in the variability of pigment composition between species. The relationships between fluorescence, chlorophyll concentration, and phytoplankton biomass are functions of light (by extinction) and also functions of the physiological status and composition of the phytoplankton community [44].

Until now, any spectral approach based on spectral data does not allow for a real separation of the phytoplankton taxa but can provide information on specific taxa clusters. The in vivo fluorescence emission of chlorophyll *a* (680 nm) arises from PSII. The light harvesting pigments in PSII are taxa specific, and thus, there are changes in the shapes of excitation spectra of the main taxa phytoplankton [17].

The in vivo excitation peak of chlorophyll *a* at 440 nm and its emission at 680 nm played an important role in the fluorescence spectra of natural phytoplankton, while the excitation wavelengths of phycocyanin in the range 550–650 nm and the emission peak around 645 nm played a major role in the fluorescence spectra of cyanobacteria [45]. The analysis of the shape of the spectrum, amplitude, and spectral position (spectral signature) can be associated with a certain phytoplankton community. The algae divisions, Dinophyta, Bacillariophyta, Chrysophyta, Cyanophyta, Cryptophyta, and Chlorophyta, are characterized by similar fluorescence excitation spectra resulting from the similar composition of their antenna pigments [46].

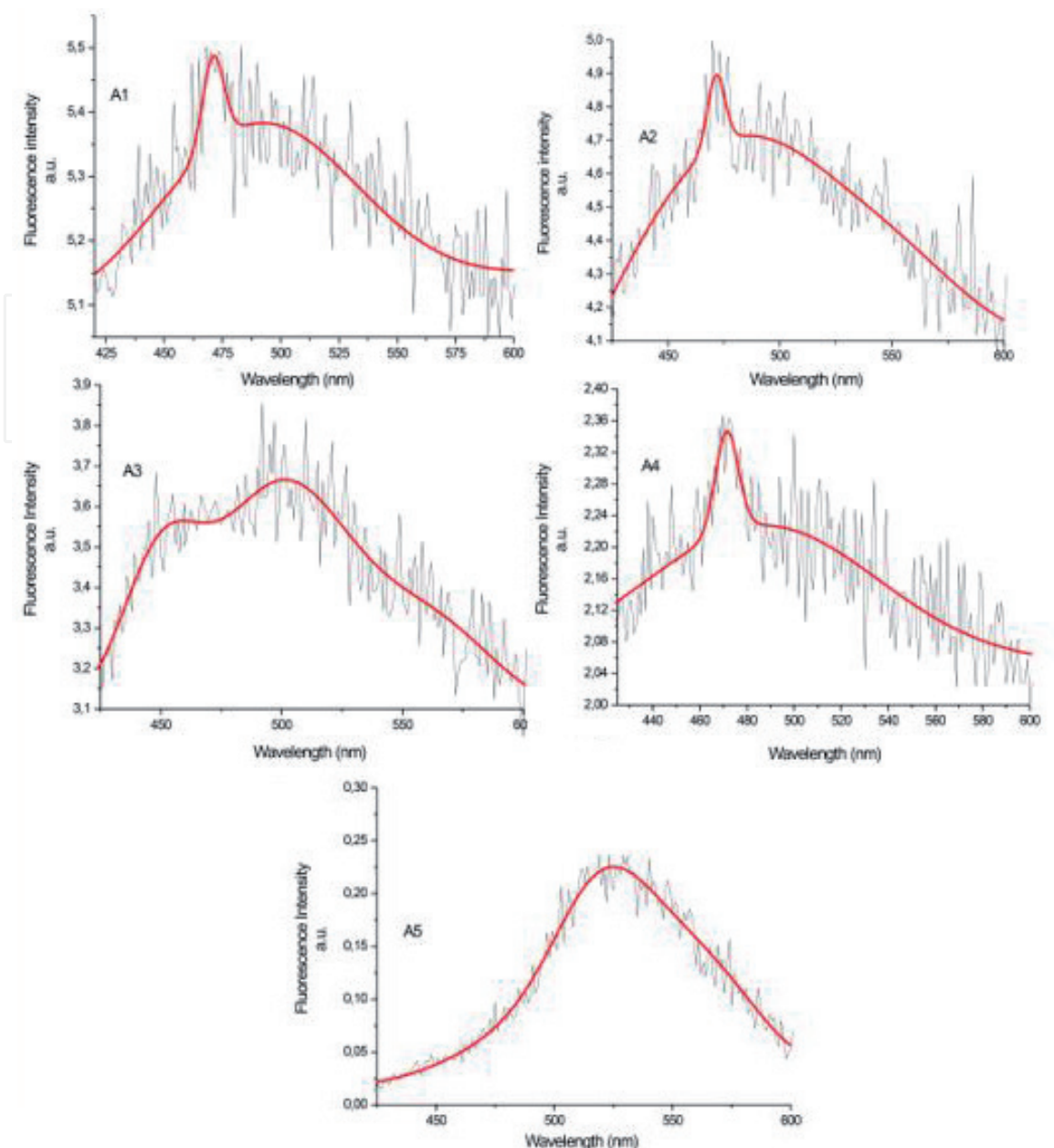### 4.2.1 Fluorescence excitation, emission spectra, and lifetime

For all taxa, light can be absorbed by chlorophyll *a* itself (440 nm); for chlorophytes also by chlorophyll *b* (480 nm) and for chromophytes by chlorophyll c (460–470 nm) and carotenoids (490–560 nm), affecting the fluorescence excitation specimen. The pigment system of cyanobacteria is however different because exhibit weak fluorescence from chlorophyll *a* but contain phycobilins that fluoresce at lower wavelengths. The cryptophytes also exhibit phycobilins and chlorophyll *a* fluorescence.

Based on the spectral behavior, it is possible to identify four major taxa groups which can be fitted with distinguishing spectra [16]: the first group is the Bacillariophyta (diatoms and dinoflagellates) which displayed in the excitation spectra a broad band with a maximum near 470 nm and a shoulder near 500 nm; the second group, chlorophyte, exhibits a spectrum similar in shape to that of the previous group but narrower. The third and fourth groups are the cryptomonads and cyanobacteria, respectively, which have similar emission due to phycobilins.

The excitation/emission spectra and lifetimes of samples A1 to A5 have been measured with a Spectrophotometer LifeSpec II. A 406 nm pulsed diode laser with excitation pulse of 80 ps was used to pump the sample contained inside a spectroscopic cuvette. The detection has been achieved with a time-correlated single-photon counting (TCSPC) detector.

In our results of fluorescence excitation spectra (**Figure 15**), we observed two emission bands for samples A1, A2, and A4, one caused by chlorophyll fluorescence with a pronounced peak centered at 475 nm and the other (a shoulder) centered at 500 nm. The ratios of fluorescence intensity (FI): FI 475/FI500 are >1 except for sample A3, which is <1, since it exhibits a different spectrum shape. Sample A5 exhibits only a large band, centered at 525 nm, identified as phycoerythrin. The emission fluorescence spectra of samples A1 and A6 are shown in **Figure 16**.

Part of the energy absorbed by the antenna pigments that is not used in the process of photosynthesis is that it can turn into fluorescent radiation.

Figure 15.
Fluorescence excitation spectra of samples A1 to A5.

Fluorescence is an important feature for identifying a specific phytoplankton taxa group. However, any change in the photosynthetic mechanism can either increase or decrease the fluorescence intensity. For example, if the antenna pigment set is affected, preventing radiation from reaching the reaction center, then fluorescence will decrease. On the other hand, the fluorescence emitted at 685 nm may increase if the antenna pigments redirect the absorbed energy to other reaction centers that will saturate, favoring fluorescence [47].

The lifetime decays of each sample (**Figure 17**) have been measured at the peak of each emission spectrum. Also, the instrumental response of the equipment (IRF) has been measured and is shown together with the decays in **Figure 17**.

The fluorescence decays are consistent with a multi-exponential equation, which can be useful to estimate an average lifetime that represents the decay rate of the system.

In order to quantify the lifetime of each sample, it has been calculated a three-exponential fitting of the decay curve (Eq. 13) that gives an estimation about the average lifetime as defined in Eq. 14:

$$I(t) = B_1 \cdot e^{(t/\tau_1)} + B_2 \cdot e^{(t/\tau_2)} + B_3 \cdot e^{(t/\tau_3)} \tag{13}$$

$$\tau_{av} = \frac{B_1 \tau_1^2 + B_2 \tau_2^2 + B_3 \tau_3^2}{B_1 \tau_1 + B_2 \tau_2 + B_3 \tau_3} \tag{14}$$

The fitting has been managed to do after a measurement data and IRF reconvolution analysis. The average lifetimes and fitting parameters are given in **Table 5**.

The measured fluorescence decay is not a simple exponential decay. It is instead a quasi-continuous exponential distribution or various distributions. This is because the pigments (for example, chlorophyll) are located in different organisms, and there is more than a single rate in the sample contributing to the fluorescence signal.
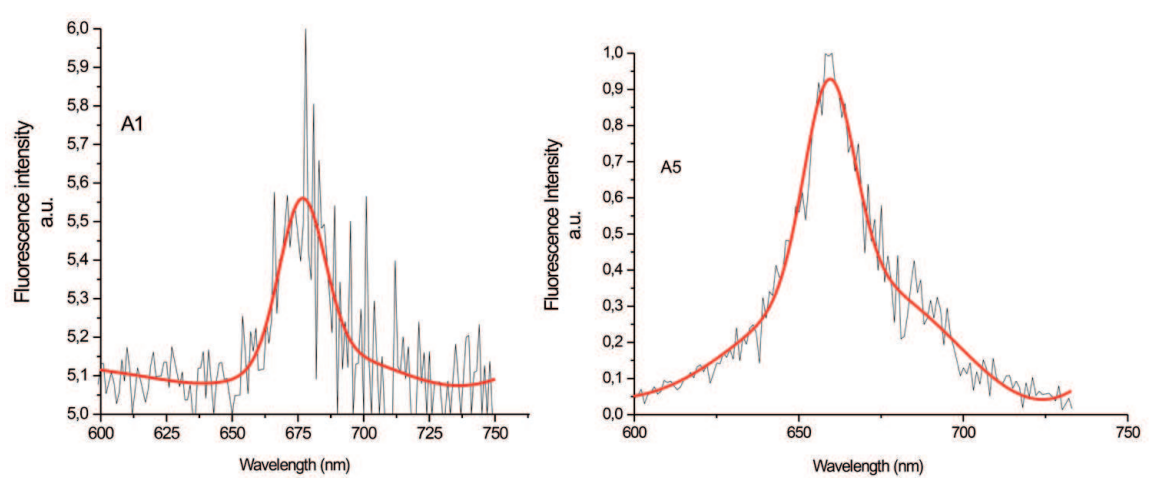
Figure 16.
Fluorescence emission spectra of samples A1 and A5.
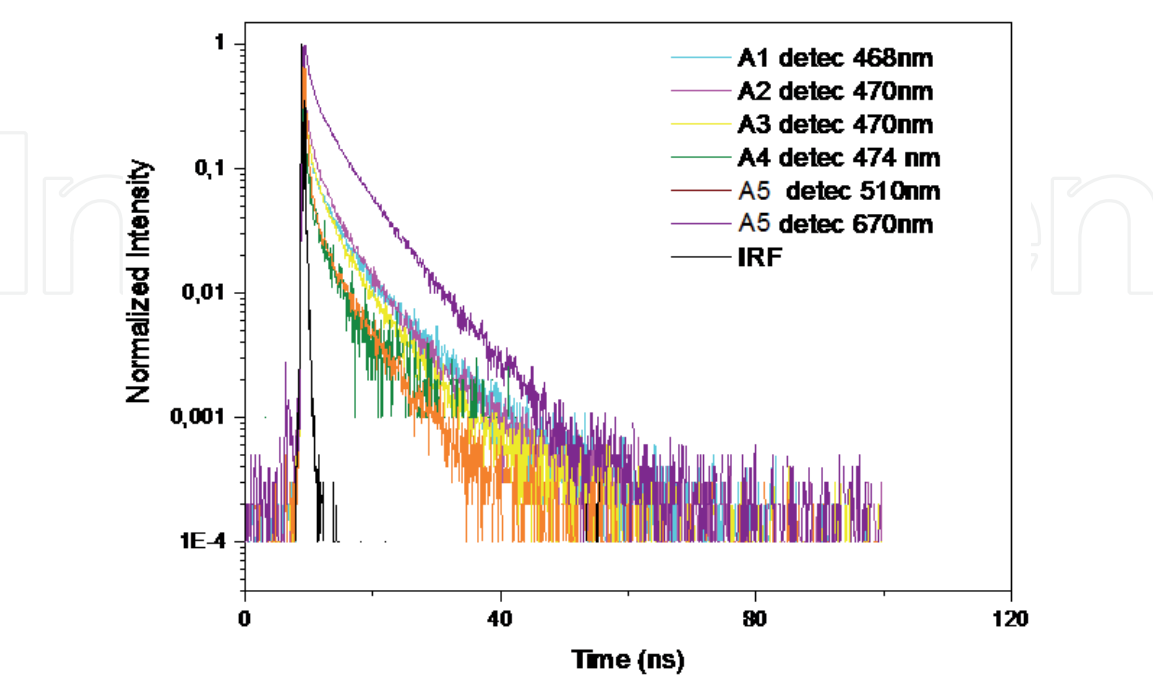
Figure 17.
Decay curves at different water samples represented distinct phytoplankton groups. IRF: instrumental response function.

23

Samples	λ_{detec} (nm)	τ_1 (ns)	τ_2 (ns)	τ_3 (ns)	B_1	B_2	B_3	τ_{av} (ns)
A1	468	0.0590	1.5440	6.5940	4.9635	0.0617	0.0253	2.2785
A2	470	0.0780	1.3160	5.3850	3.0872	0.0938	0.0401	2.3166
A3	470	0.0690	1.2410	5.0870	3.7274	0.0753	0.0308	1.8346
A4	474	0.0390	0.0650	2.2820	0.0111	4.4557	0.0351	0.5447
A5	510	0.0800	0.5340	4.2390	3.4867	0.1410	0.0201	0.9642
	670	0.1990	1.5170	6.1320	0.9297	0.1910	0.1343	4.2566

Table 5.
Fluorescence lifetime values for the different water samples represented distinct phytoplankton groups.

Acknowledgements

Conflict of interest

The authors declare no conflict of interest.

Author details

Helena C. Vasconcelos[1,2]*, Joao A. Lopes[3], Maria João Pereira[1,4]
and Afonso Silva Pinto[5]

1 Science and Technology Faculty (FCT), University of the Azores,
Ponta Delgada, Azores, Portugal

2 CEFITEC, Center for Physics and Technological Research, Faculty of Science and Technology (FCT), New University of Lisbon, Lisbon, Portugal

3 Research Institute for Medicines (iMed.ULisboa), Faculty of Pharmacy, University of Lisbon, Lisbon, Portugal

4 Biotechnology Centre of Azores, Ponta Delgada, Azores, Portugal

5 Innovation Green Azores (IGA), Ponta Delgada, Azores, Portugal

*Address all correspondence to: helena.cs.vasconcelos@uac.pt

IntechOpen

References

[1] Cruz J, Pacheco D, Porteiro J, Cymbron R, Mendes S, Malcata A, et al. Analysis of long-term monitoring data and remediation measures. Science of The Total Environment. São Miguel, Azores: Sete Cidades and Furnas lake eutrophication; 2015:520. DOI: 10.1016/j.scitotenv.2015.03.052

[2] Oliver R, Ganf G. Freshwater blooms. In: Whitton B, Potts M, editors. The Ecology of Cyanobacteria: Their Diversity in Time and Space. The Netherlands: Kluwer Academic Publishers; 2000. pp. 149-194

[3] LL/SMG, 2013-2016. Book of the Ponds. Available from: https://servicos-sraa.azores.gov.pt/grastore/DRA/RH/Book-Lagoas-SMG-2013-2016.pdf [Accessed: 25 March 2020]

[4] Allakhverdiev SI, Kreslavski VD, Zharmukhamedov SK, et al. Chlorophylls d and f and their role in primary photosynthetic processes of cyanobacteria. Biochemistry (Moscow). 2016;**81**:201-212. DOI: 10.1134/S0006297916030020

[5] Telfer A. Too much light? How beta-carotene protects the photosystem II reaction centre. Photochemical & Photobiological Sciences: Official Journal of the European Photochemistry Association and the European Society for Photobiology. 2006;**4**:950-956. DOI: 10.1039/b507888c

[6] Santos-Ballardo D, Rossi S, Hernández V, Vázquez R, Unceta C, Caro-Corrales J, et al. A simple spectrophotometric method for biomass measurement of important microalgae species in aquaculture. Aquaculture. 2015;**448**:87-92. DOI: 10.1016/j.aquaculture.2015.05.044

[7] Escoffier N, Bernard C, Hamlaoui S, Groleau A, Catherine A. Quantifying phytoplankton communities using spectral fluorescence: The effects of species composition and physiological state. Journal of Plankton Research. 2015;**37**(1):233-247. DOI: 10.1093/plankt/fbu085

[8] Beutler M, Wiltshire KH, Meyer B, Moldaenke C, Luring C, Meyerhofer M, et al. A fluorometric method for the differentiation of algal populations in vivo and in situ. Photosynthesis Research. 2002;**72**:39-53

[9] Millie DF, Schofield OME, Kirkpatrick GJ, Johnsen G, Evens TJ. Using absorbance and fluorescence spectra to discriminate microalgae. European Journal of Phycology. 2002;**37**:313-322

[10] Krause GH, Weis E. Chlorophyll fluorescence and photosynthesis: The basics. Annual Review of Plant Physiology and Plant Molecular Biology. 1991;**42**:313-349

[11] Kirkpatrick G, Millie DF, Moline MA, Schofield O. Absorption-based discrimination of phytoplankton species in naturally mixed populations. Limnology and Oceanography. 2000;**42**:467-471

[12] Bricaud A, Babin M, Morel A, Claustre H. Variability in the chlorophyll-specific absorption coefficients of natural phytoplankton: Analysis and parameterization. Journal of Geophysical Research. 1995;**100**(C7):13321-13332

[13] Ciotti AM, Lewis MR, Cullen JJ. Assessment of the relationships between dominant cell size in natural phytoplankton communities and the spectral shape of the absorption coefficient. Limnology and Oceanography. 2002;**47**(2):404-417

[14] Available from: http://algaevision.myspecies.info/node/3510

[15] Rodhe W. Crystallization of eutrophication concepts in North Europe. In: Eutrophication, Causes, Consequences, Correctives. Washington D.C.: National Academy of Sciences; 1969. pp. 50-64

[16] Yentsch CS, Phinney DA. Spectral fluorescence: An ataxonomic tool for studying the structure of phytoplankton populations. Journal of Plankton Research. 1985;**7**(5):617-632. DOI: 10.1093/plankt/7.5.617

[17] Yentsch CS, Yentsch CM. Fluorescence spectral signatures: The characterization of phytoplankton populations by the use of excitation and emission spectra. Journal of Marine Research. 1979;**37**:471-483

[18] MacIntyre HL, Lawrenz E, Richardson TL, Suggett DJ, et al. Taxonomic discrimination of phytoplankton by spectral fluorescence. In: Chlorophyll a Fluorescence in Aquatic Sciences: Methods and Applications, Developments in Applied Phycology. Vol. 4. Dordrecht: Springer; 2010. pp. 129-169

[19] Seppälä J. Spectral absorption and fluorescence characteristics of the Baltic Sea phytoplankton. ICES CM. 2003;**50**:2-6

[20] Sathyendranath S, Lazzara L, Prieur L. Variations in the spectral values of specific absorption of phytoplankton. Limnology and Oceanography. 1987;**32**:403-415

[21] Jolliffe I. Principal component analysis. In: Lovric M, editor. International Encyclopedia of Statistical Science. Berlin, Heidelberg: Springer; 2011

[22] Erdmann R, Enderlein J, Wahl M. Time Correlated Single-Photon Counting and fluorescence Spectroscopy. 2005

[23] Lakowicz JR. Principles of Fluorescence Spectroscopy. 3rd ed. New York: Springer; 2006

[24] van Holde KE, Johnson WC, Ho PS. Principles of Physical Biochemistry. 2nd ed. Upper Saddle River, NJ: Prentice Hall; 1998

[25] Demas JN. Excited State Lifetime Measurements. New York: Academic Press; 1983

[26] Connor DVO, Philips D. Time Correlated Single Photon Counting. London: Academic Press; 1984

[27] Birch DJS, Imhof R. In: Lakowicz JR, editor. Topics in Fluorescence Spectroscopy. Vol. 1. New York: Plenum Press; 1991

[28] Antunes P, Rodrigues FC. Azores volcanic lakes: Factors affecting water quality. Water Quality: Current Trends and Expected Climate Change Impacts. 2011;**348**:106-114

[29] Andrade C, Viveiros F, Cruz JV, Coutinho R, Silva C. Estimation of the CO_2 flux from Furnas volcanic Lake (São Miguel, Azores). Journal of Volcanology and Geothermal Research. 2016;**315**:51-64. DOI: 10.1016/j.jvolgeores.2016.02.005

[30] Santos M, Muelle H, Pacheco D. Cyanobacteria and microcystins in lake Furnas (S. Miguel Island-Azores). Limnetica. 2012;**29**:107-118

[31] Wetzel RG. Limnologia. Lisboa: Fundação Calouste Gulbenkian; 1993. p. 919

[32] Available from: http://www.azores.gov.pt/Portal/pt/entidades/sraf/noticias/Governo+dos+A%C3%A7ores+anuncia+medidas+de+combate+%C3%A0+eutrofiza%C3%A7%C3%A3o+na+Lagoa+das+Furnas.htm

[33] Available from: https://www.publico.pt/2016/03/23/ecosfera/

noticia/acores-lancam-obra-para-combater-a-eutrofizacao-da-lagoa-das-furnas-1726994

[34] Available from: https://www.aprh.pt/congressoagua2002/pdf/p20.pdf

[35] Available from: https://www.acorianooriental.pt/noticia/regiao-destaca-esforco-no-combate-a-eutrofizacao-nas-lagoas-294433

[36] Available from: https://www.azores.gov.pt/Gra/srrn-drotrh/menus/principal/Monitorização/

[37] Available from: https://www.edinst.com/products/lifespec-ii-dedicated-lifetime-spectrometer/

[38] Available from: https://www.edinst.com/blog/what-is-tcspc/

[39] Valeur B, Berberan-Santos MN. In: Valeur B, editor. Molecular Fluorescence: Principles and Applications. Weinheim, Germany: Wiley-VCH Verlag GmbH; 2001. ISBNs: 3-527-29919-X (Hardcover); 3-527-60024-8 (Electronic)

[40] Paul WJ, Hamilton DP, Ostrovsky I, Miller SD, Zhang A, Muraoka K. Catchment land use and trophic state impacts on phytoplankton composition: A case study from the Rotorua lakes' district, New Zealand. In: Salmaso N, Naselli-Flores L, Cerasino L, Flaim G, Tolotti M, Padisák J, editors. Phytoplankton Responses to Human Impacts at Different Scales. Developments in Hydrobiology. Vol. 221. Dordrecht: Springer; 2012

[41] Jensen JP, Jeppesen E, Kristensen P, Christensen PB, Søndergaard M. Nitrogen loss and denitrification as studied in relation to reductions in nitrogen loading in a shallow, hypertrophic lake (Lake Søbygård, Denmark). Internationale Revue der Gesamten Hydrobiologie. 1992;**77**:29-42

[42] Jeppesen E, Søndergaard M, Jensen JP, Havens KE, Anneville O, Carvalho L, et al. Lake responses to reduced nutrient loading – An analysis of contemporary long-term data from 35 case studies. Freshwater Biology. 2005;**50**:1747-1771. DOI: 10.1111/j.1365-2427.2005.01415.x

[43] Moed J, Hallegraeff G. Some problems in the estimation of chlorophyll-a and phaeopigments from pre and post-acidification spectrophotometrie measurements. International Review of Hydrobiology. 1978;**63**:787-800. DOI: 10.1002/iroh.19780630610

[44] Dickey TD. Recent advances and future directions in multi-disciplinary in situ oceanographic measurement systems. In: Rotllsoiild BJ, editor. Toward a Theory of Biological Physical Interactions in the World Ocean. Dordrecht, The Netherlands: Kluwer Academic; 1988. pp. 555-598

[45] Campbell D, Hurry V, Clarke A, Gustafsson P, Oquist G. Chlorophyll fluorescence analysis of cyanobacterial photosynthesis and acclimation. Microbiology and Molecular Biology Reviews: MMBR. 1998;**62**:667-683. DOI: 10.1128/MMBR.62.3.667-683.1998

[46] Roy S, Llewellyn C, Egeland E, Johnsen G, editors. Phytoplankton Pigments: Characterization, Chemotaxonomy and Applications in Oceanography (Cambridge Environmental Chemistry Series). Cambridge: Cambridge University Press; 2011. DOI: 10.1017/CBO9780511732263

[47] Falkowski PG, Kolber Z. Variations in chlorophyll fluorescence yields in phytoplankton in the world oceans. Australian Journal of Plant Physiology. 1995;**22**:341-355